RESEARCH ARTICLE

SERS Detection of Hg^{2+} using Rhenium Carbonyl Labelled Nanoparticle Films

Joshua N. Lea,[a] Heather J. Montgomery,[b] Yikai Xu[b], Steven E. J. Bell[b], Lorna Ashton,[a] and Nicholas C. Fletcher[a]*

[a] Dr. J. N. Lea, Dr. L. Ashton, and Dr. N. C. Fletcher
Department of Chemistry Lancaster University, Bailrigg, Lancaster, LA1 4YB, UK. Email: n.fletcher@lancaster.ac.uk
Lancaster University
Bailrigg, Lancaster, LA1 4YB, UK
E-mail: n.fletcher@lancaster.ac.uk

[b] Dr. H. J. Montgomery, Dr. Y.i Xu, Prof. S. E. J. Bell
School of Chemistry and Chemical Engineering
Queen's University Belfast
David Keir Building, Belfast, Northern Ireland, BT9 5AG, UK

Supporting information for this article is given via a link at the end of the document.

Abstract: Modified silver nanoparticles with a self-assembled disulfide functionalized 2,2´-bipyridine (L1 and L2) monolayer, and the corresponding rhenium complex $[Re(L2)(CO)_3Br]$ are shown to provide a method to position the nanoparticles at a water/dichloromethane interface forming a lustrous metal-like-liquid film (MeLLF) with a unique SERs response. The film formed using L2 showed divergent behavior in the presence of a range of metal ions whilst bound to the surface. $[Re(L)(CO)_3Br]$ (where L = 2,2´-bipyridine, L1 and L2) in solution demonstrates a selective interaction with Hg^{2+}, observed by UV-vis, emission and ^1H NMR spectroscopy, attributed to abstraction of the bromide. This interaction was demonstrated by subtle changes in the characteristic Raman Re-CO stretch at 510 cm^{-1} both with the MeLLF, and when the film is immobilized in a PVA surface-exposed-nano-sheet (SENS). The work provides proof of concept that the organometallic complexes can be employed as "labels" to generate SERS-active nanoparticle films that possess detection capabilities.

Introduction

Surface-enhanced Raman spectroscopy (SERS) offers a non-destructive and highly sensitive approach to analytical sensing with claimed detection limits reaching single molecule levels.[1] Amplification of a molecule's Raman response can be achieved by both electromagnetic (EM) and charge-transfer (CT) mechanisms between the molecule and a roughened metal surface.[2] The EM mechanism relies on the excitation of the localized plasmonic resonances, with noble metal nano-scaled structures possessing absorption in the visible to near infrared region. Consequently, aggregated nanoparticles provide considerable SERS amplification, with the contact zones between individual particles being described as "hotspots".[3] This has a significant advantage over other analytical techniques such as UV-Vis and fluorescence spectroscopy as it provides both substrate specific vibrational information, as well as enhanced sensitivity. However, designing simple, ordered, and reproducible aggregated nanoparticles with high selectivity remains a challenge.[4]

Common approaches for SERS-based sensing involve "label-free" interactions where recognition of the Raman fingerprint is achieved via adsorption of the analyte directly onto a pre-prepared surface, often following competitive displacement of the species stabilizing the surface such as citrate. Such systems have shown application for the detection of trace amounts of a wide range of analytes including illegal drugs, biological markers and environmental pollutants.[5] But in multicomponent samples, there is little analyte selectivity as adsorption can be a nonspecific process, leading to very complicated spectra, especially within the biological or "fingerprint region" (1500 to 600 cm^{-1}). Labelled surfaces, where sensing is achieved via observable changes in the Raman spectrum of a secondary reporting function, or "label", can offer far greater analyte selectivity. Recent examples have been used to identify significant environmental pollutants such as As^{3+}[6], and Hg^{2+} in black tea.[7]

Diimine organometallic complexes of the late transition metals based on $[Ru(bpy)_3]^{2+}$, $[Ir(ppy)_3]$ and $[Re(bpy)(CO)_3X]$ (where X is a halide or other monodentate ligand) have been widely used as fluorescent sensors.[8] They offer high photostability and versatility as their photophysical and target binding properties can be tuned through ligand design and have been shown to retain these properties when bound to gold nanoparticles.[9] The Yam and co-workers have previously demonstrated that esterase activity can release these species from a gold nanoparticle resulting in enhanced emission.[10] These complexes also have a significant Raman response due to resonance enhancement arising from their long-lived triplet states. Yet they have seen limited investigation as possible SERS labels despite the potential to drive sensitivity to even greater levels through surface-enhanced resonance Raman spectroscopy (SERRS). Previously, we have reported the synthesis of a *fac*-$[Re(L1)(CO)_3Br]$ complex (Scheme 1) that demonstrated a remarkably sensitive SERRS response on aggregated Ag nanoparticles,[11] although we are yet to illustrated this system as a selective detection platform. These Re(I) complexes present metal carbonyl vibrational modes (Re–CO stretch at 510 cm^{-1} and ReC=O stretches around 1910 and 2025 cm^{-1}) outside the conventional organic Raman window, as also shown by Pérez-Mirabet *et al*. by the coordination of $\{Re(CO)_3\}$ to 3-

mercaptopropionic acid stabilized gold and silver nanoparticles.[12] This permits detection of targeted analytes against an environmental background. A similar approach has recently been adopted using a tri-osmium-carbonyl clusters with sensitivity for glucose,[13] the Epstein-Barr virus, and tumor-related DNA.[14]

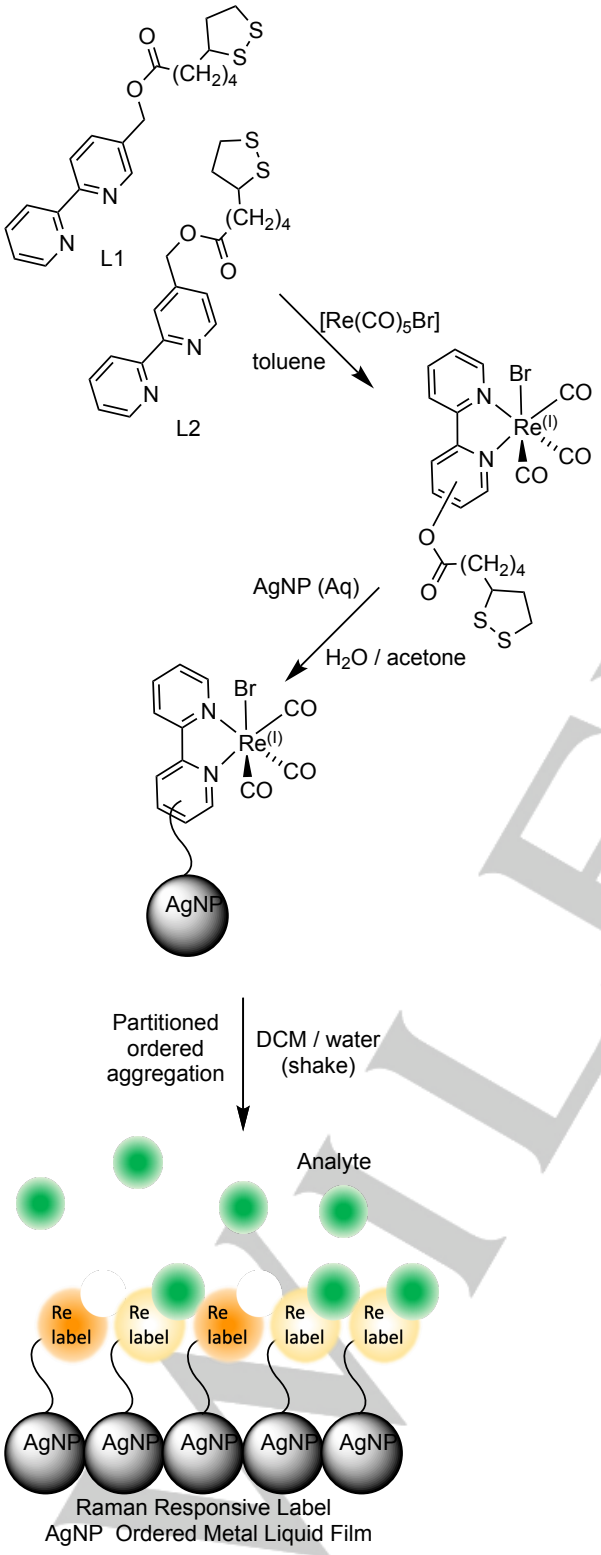

Scheme 1. Formation of Rhenium labelled Raman responsive Metal-like-liquid Film (MELF).

The challenge is now to take the selective sensing demonstrated in the laboratory under controlled conditions, into the real world. The current limitations for developing SERS labelled substrates is the reproducible fabrication of a roughened, highly ordered, nanoscale substrate, suitable to be transposed into a portable device.[15] One possible bottom-up approach is to exploit an interfacial nanoparticle film. Nanoparticles can readily be suspended at a water-oil interface, using relatively cheap materials with high reproducibility in both fabrication and the SERS activity.[16] These metal liquid-like films, or MeLLFs, can be formed via surface modification using a molecule that binds to the nanoparticle increasing the hydrophobicity, leading to a monolayer partitioned between the two immiscible solvents.[17] Film formation can also be achieved by screening the surface charge of the nanoparticle using amphiphilic salts stabilizing the potential on both sides of the interface.[18] Both approaches result in stable and reproducible surfaces that offer high levels of SERS enhancement. An additional advantage is that film formation requires less than 5 ml quantities of a standard suspension of citrate stabilized silver nanoparticles (AgNPs)[19] and microlitre portions of the modifying/promoting reagent. These films have already seen application for label-free detection of heavy metals, pesticides, and serum creatinine.[20]

We demonstrate here a method that extends the application of interfacial films to labelled SERS sensing using a Re(I) complex that acts as both modifier, and detection platform. This new modular approach of forming labelled interfacial nanoparticle films uses a straightforward process and demonstrates an application as a SERS sensor (Scheme 1). By incorporating both substrate formation and SERS-labelling into one specific step, we minimize the requirement for complex multi-step processes without sacrificing reproducibility and we demonstrate here a system with remarkable selectivity for aqueous mercuric salts.

Results and Discussion

L2 metal cation response

Thiols have been successfully employed to functionalize and suspend noble metal nanoparticles at a water/oil interface,[17, 21] and our earlier work described the successful bulk aggregation of AgNPs with the disulfide functionalized bipyridyl ester L1

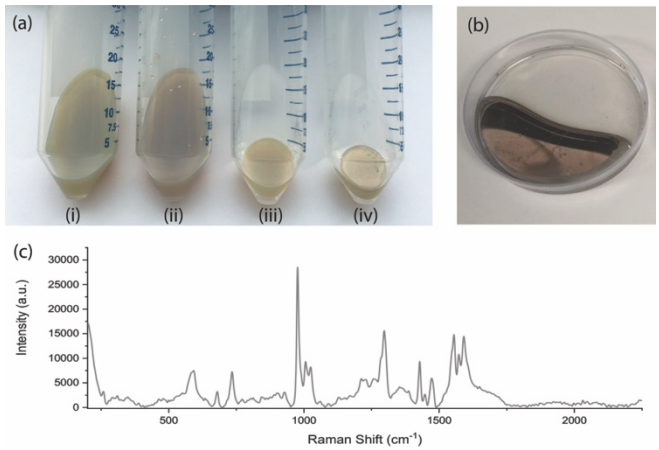

Figure 1 (a) A photograph of (i) colloidal AgNP, (ii) colloidal AgNP with L2, (iii) colloidal AgNP@L2 layered on DCM, (iv) colloidal AgNP@L2 layered on DCM after shaking showing the MeLLF has formed. (b) The MeLLF after transfer into a petri dish and (c) the SERS spectrum of the Ag@L2 MeLLF.

(Scheme 1).[11] To explore whether highly ordered interfacial films could be made using such ligands, L2 was prepared using an adapted procedure via esterification of 4-hydroxymethyl-2,2′-bipyridine with thioctic acid (Scheme 1, Supp. Figure 1). Previously, studies had focused on ligand L1, with the appended functionalization at the 5 position.[11] But it had been noticed that the relative orientation of the bipyridyl group with respect to the surface, varied with concentration. It was hoped that this could be limited by moving the thiolated group to the 4 position.

Addition of a small aliquot of a 1 mM acetone solution of L2 to an aqueous suspension of citrate-stabilized nanoparticles caused an observable color change to the nanoparticle suspension, suggesting L2 had bound to the surface (Figure 1a). Film formation was realized upon vigorous shaking of the nanoparticle solution in the presence of dichloromethane, giving the characteristic metallic luster of a MeLLF. The Raman spectrum of the resulting film (irradiated at 785 nm) displayed the anticipated bands associated with the bipyridyl and the thiolated tether (Figure 1c). The prominent bands appearing at 616, 997, and 1024 cm^{-1} correspond to aliphatic C–S stretching, aromatic ring breathing and ring–ring stretch respectively, which are in good agreement with the previously reported bulk aggregation of L1 with AgNPs.[11, 22]

2,2′-Bipyridine has well documented coordination to most metal cations. Metal perchlorate salts of Hg^{2+}, Pb^{2+}, Zn^{2+}, Fe^{2+} and Co^{2+} were added to freshly prepared AgNP@L2 MeLLFs without appearing to impact the stability of the film. Each metal presents its own chelation requirements to the diimine, arising from the cation size and charge, the degree of π-donation from the metal to the aromatic π^* orbitals, and the restriction in the free rotation along the inter-ring bond. This will be reflected in the bond and torsion angles in the five atom chelate, resulting in metal specific variation in the ring breathing bands at 995 cm^{-1}, and the inter-ring stretch in the region of 1024 cm^{-1}.[23] Raman spectroscopy of the treated films display a number of changes to these peaks (Figure 2, Supp. Table 1). It was observed that the large cations Hg^{2+} and Pb^{2+} offer subtle changes in the Raman response, with Hg^{2+} causing a peak at 1008 cm^{-1} whilst Pb^{2+} shows a decrease in the intensity of the 1024 cm^{-1} peak, and the appearance of a new peak at 1190 cm^{-1}. Conversely, the presence of Zn^{2+} causes a dramatic increase in intensity of the ring–ring stretch at 1023 cm^{-1}. Both Co^{2+} and Fe^{2+} cause the appearance of strong vibrations at 1033 cm^{-1} and a decrease in the ring breathing mode at 997 cm^{-1} consistent with metal coordination. The presence of Fe^{2+} also sees the addition of a new peak at 1485 cm^{-1} assigned to Fe-bpy vibration.[24] Given these subtle differences, there is evidence that AgNP@L2 interfacial films can potentially be used to show discrimination between cations using SERS.

Film formation with [Re(L2)(CO)$_3$Br]

Thioctic (lipoic) acid derivatives have previously shown to be suitable components to tether [Re(L1)(CO)$_3$Br] to AgNPs (Scheme 1).[11] [Re(L2)(CO)$_3$Br] was synthesized in a similar fashion by refluxing L2 with [Re(CO)$_5$Br] in toluene (Supp. Figure 2).[11] Subsequent addition of a dilute acetone solution containing the resulting complex to citrate-stabilized silver nanoparticles results in a color change from green/yellow to brown (Supp Figure 3). MeLLF formation is achieved by shaking the aqueous suspension with DCM until a mirror-like appearance is observed at the interface between the two immiscible solvents. The Raman spectrum of the resulting film (Figure 3a) displays the

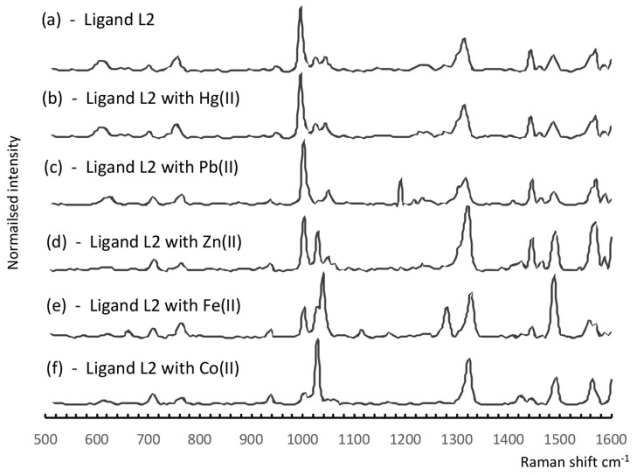

Figure 2 The SERS response of the AgNP@L2 MeLLF film after washing with different metals, (a) Blank, (b) $Hg(ClO_4)_2$, (c) $Pb(ClO_4)_2$, (d) $Zn(ClO_4)_2$, (e) $Fe(ClO_4)_2$, and (f) $Co(ClO_4)_2$.

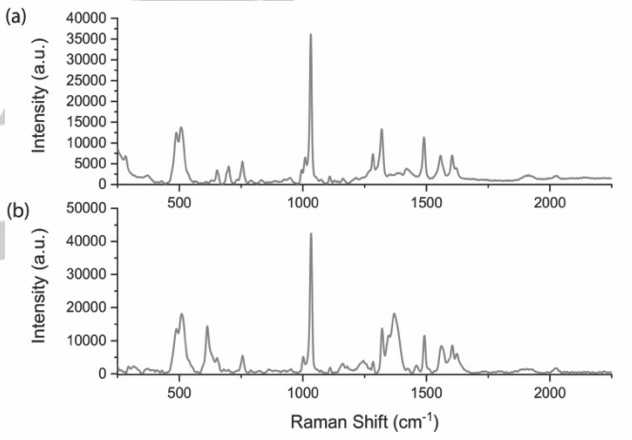

Figure 3 The SERS spectra of (a) the Ag@[Re(L2)(CO)$_3$Br] MeLLF and (b) the Ag@[Re(L2)(CO)$_3$Br] SENS showing remarkable similarities.

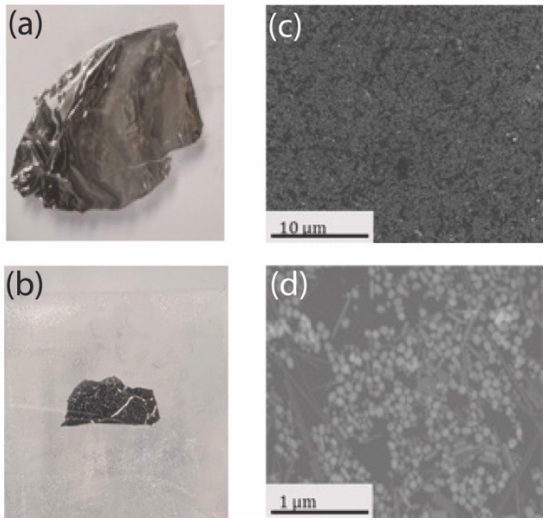

Figure 4 (a) Image of Ag@[Re(L2)(CO)$_3$Br] SENS floating on water and (b) isolated on sticky tape. (c) and (d) are SEM images of the film, showing the individual silver nanoparticles.

characteristic peaks anticipated for the complex [Re(L2)(CO)$_3$Br] with the Re–C stretch at 510 cm^{-1} and the weak metal carbonyl signals at 1910 and 2025 cm^{-1}.[11] The vibrations corresponding to the bipyridyl and thioctic groups are also apparent.

Given the fluid nature of a MeLLF, it presents several problems as a detection surface, particularly with respect to transportation, handling and long-term stability. This can be overcome by the inclusion of a dissolved polymer within the dichloromethane layer during the formation of the film, as previously demonstrated by Xu.[25] Slow evaporation of the volatile solvent results in one side of the MeLLF being embedded in a thin solid polymer layer, previously described as a surface-exposed nanosheet or SENS.[26] These materials mirror the advantageous SERS enhancement of MeLLFs, but are far more robust and are more easily manipulated.

[Re(L2)(CO)$_3$Br] SENS were formed using a procedure adapted from the literature.[25] A suspension of AgNPs modified with [Re(L2)(CO)$_3$Br] were shaken in the presence of a DCM solution of polystyrene until a metallic luster confirmed interfacial positioning. This was transferred to a petri dish and sealed until the film had ordered itself and then left to dry. The resulting film could be cut and transferred onto sticky tape. Scanning electron microscopy of the resulting AgNP@[Re(L2)(CO)$_3$Br] SENS shows individual nanoparticles suspended in the polymer layer (Figure 4). The Raman spectrum of the SENS is remarkably similar to the MeLLF analogue and possesses the key vibrational characteristics of the Re centre (509, 1900 and 2020 cm^{-1}), the bipyridyl group (1034 cm^{-1}) and the thioctic tether (654 cm^{-1}) (Figure 3b). Whilst there are weak signals resulting from the polystyrene, it confirms that the aqueous Re-modified surface remains exposed and potentially available as a labelled sensing platform.

Optical Response to Hg^{2+}

Sensing of Hg^{2+} is of considerable importance from both an environmental and a physiological perspective.[27] Strategies based around nanomaterials have drawn particular attention.[28] These include a series of articles indicating that the detection of Hg^{2+} can be achieved by the loss of color from AgNPs stabilized by citrate,[29] p-phenylenediamine,[30] cysteamine,[31] PVA[32] and a range of biologically derived compounds[33] with the bleaching of the plasmonic resonance attributed to the selective reduction of Hg^{2+} by the Ag nanoparticle and potentially amalgamation with the nanoparticle surface. Hg^{2+} has also been detected through fluorescent enhancement with a AgNP bound rhodamine B derivative.[34] However, as a spherical single cation, it does not readily lend itself to detection by vibrational techniques, and so the possibilities ultrasensitive detection that SERS can offer must rely on indirect reporting. A variety of “labels” bound to a nanostructured surface have been considered.[35] These include the use of a cystine labelled DNA aptamer bound to a AgNP,[36] as well as displacement strategies giving a Raman “turn off” response by surface stripping, for example, 4-amionothiol from a AgAu alloy NP,[7] 4-mercaptobenzoic acid from a nano-porous Au substrate,[37] 4,4´-bipyridine[38] or phenylacetylene[39] from AgNPs.

Rhenium complexes have previously been considered as sensors that display observable changes to their UV-vis and emission response with a wide variety of analytes including anions, as well as reporting on various biological environments.[40] [Re(L)(CO)$_3$Br] (where L is bpy, L1 and L2) display the anticipated UV-vis absorbance and emission behavior presenting a π–π* ligand centered absorption at approximately 290 nm and a metal-to-ligand-charge-transfer (MLCT) absorption at in the region of 380 nm, and an emission at 600 nm (Supp. Figure 4 and Supp. Table 2).[41] Surprisingly, it was noted that the addition of mercuric salts to these rhenium complexes resulted in a noticeable change in both color and emission from the triplet metal to ligand charge transfer (^{3}MLCT) excited state; an observation of a recognition event that could potentially be exploited using the labelled AgNP films.

To quantify the spectroscopic behavior of [Re(L)(CO)$_3$Br] (where L is bpy, L1 and L2), a range of metal perchlorate salts were introduced to acetonitrile solutions of the three complexes (Figure 5). There was no significant perturbation in either the absorption, or the emission spectra with Pb^{2+}, Cd^{2+}, Zn^{2+}, Cu^{2+}, Ni^{2+}, Fe^{2+}, Co^{2+}, and Ag^{+} (Supp. Figure 5). But with introduction of mercuric perchlorate, the absorption shows a noticeable blue shift in both the π–π* and the MLCT transitions, coupled with an increase in the emissive quantum yield (Figure 5b, Supp. Figure 6 & 7). Mercuric nitrate salts were also noted to induce a similar response to both the UV-vis absorption and emission spectra (Supp. Figure 8-10). However, in acetone, rather than acetonitrile, the introduction of Hg^{2+} results in almost complete quenching of the emission (Supp. Figure 11). It is possible that this could arise from the introduction of a new electron transfer process but given the considerable change in the ground state spectrum and the variation in behavior within different media, this suggests that there is a chemical change, and that the solvent is involved giving this remarkably selective colorimetric response. It was also observed that trace amounts of water also influenced the system.

Sequential addition of $Hg(ClO_4)_2$ to [Re(L)(CO)$_3$Br] (where L represents bpy, L1 and L2) in D$_3$-acetonitrile similarly resulted in considerable changes to the ^{1}H NMR spectra of the complexes. A number of peaks see a decrease in intensity as a set of new peaks grow in with increasing Hg^{2+} concentration. An observed stoichiometry of two rhenium complexes to one Hg^{2+} cation (Supp. Figure 12-14) was evident. This behavior was not observed upon the introduction of other metal perchlorate salts, confirming that the presence of Hg^{2+} aids in the formation of a new species. The changes in the spectra are more complicated on the introduction of $Hg(NO_3)_2$ (Supp. Figure 15-17) with initial changes being consistent with the behavior seen with the metal perchlorate salt. However, as $Hg(NO_3)_2$ concentration increases, the compound converts to a third species and precipitation is observed. This suggests that mercuric salts readily, and irreversibly, abstract the coordinated bromide at room temperature, leaving a vacant site that then accepts an appropriate solvent, which over time will then coordinate to nitrate forming an insoluble neutral species (Scheme 2).

$$Hg^{2+} + 2[Re(L)(CO)_3Br] + CH_3CN \longrightarrow HgBr_2(s) + 2[Re(L)(CO)_3(CH_3CN)]^+$$

$$[Re(L)(CO)_3(CH_3CN)]^+ + NO_3^- \longrightarrow [Re(L)(CO)_3(NO_3)](s) + CH_3CN$$

Scheme 2 Proposed reaction between [Re(L)(CO)$_3$Br] and $Hg(NO_3)_2$

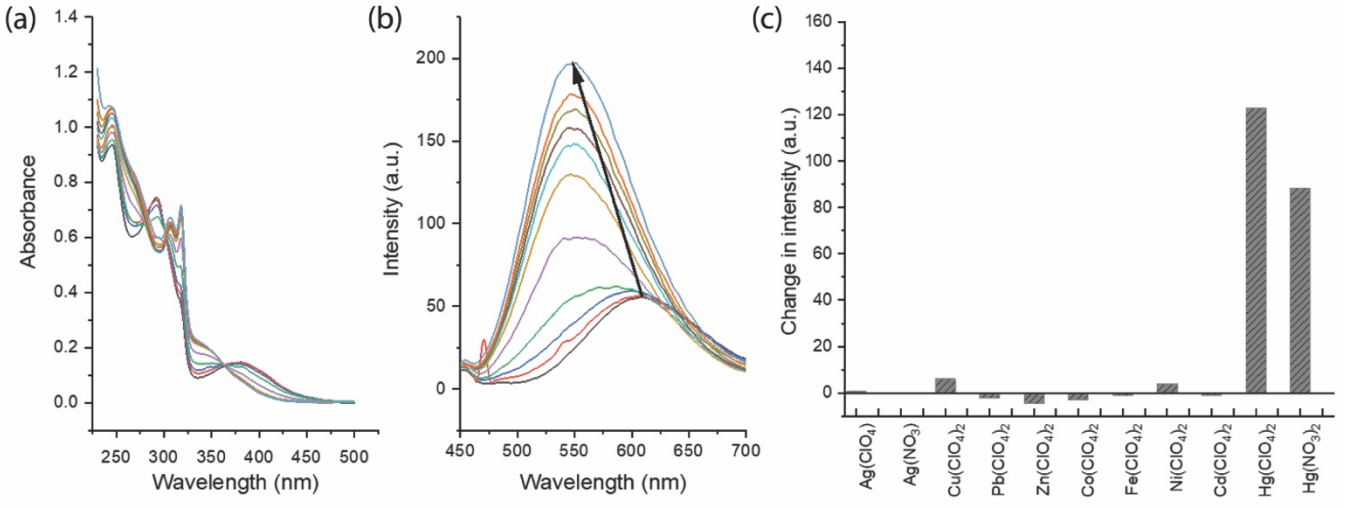

Figure 5 The UV-vis (a) and emissive (b) spectroscopic response of the [Re(L2)(CO)$_3$Br)] complex to the titration of Hg(ClO$_4$)$_2$ using molar equivalents 0.0 (–), 0.2 (–), 0.4 (–), 0.6 (–), 0.8 (–), 1.0 (–), 1.5 (–), 2.0 (–), 3.0 (–), 5.0 (–), 10.0 (–) in acetonitrile. (c) The observed change in emission intensity after addition of 10 molar equivalents of the metal perchlorate salts. Emission spectra were excited at 400 nm.

Sequential addition of Hg(ClO$_4$)$_2$ to [Re(L)(CO)$_3$Br] (where L represents bpy, L1 and L2) in D$_3$-acetonitrile similarly resulted in considerable changes to the ^{1}H NMR spectra of the complexes. A number of peaks see a decrease in intensity as a set of new peaks grow in with increasing Hg^{2+} concentration. An observed stoichiometry of two rhenium complexes to one Hg^{2+} cation (Supp. Figure 12-14) was evident. This behavior was not observed upon the introduction of other metal perchlorate salts, confirming that the presence of Hg^{2+} aids in the formation of a new species. The changes in the spectra are more complicated on the introduction of Hg(NO$_3$)$_2$ (Supp. Figure 15-17) with initial changes being consistent with the behavior seen with the metal perchlorate salt. However, as Hg(NO$_3$)$_2$ concentration increases, the compound converts to a third species and precipitation is observed. This suggests that mercuric salts readily, and irreversibly, abstract the coordinated bromide at room temperature, leaving a vacant site that then accepts an appropriate solvent, which over time will then coordinate to nitrate forming a neutral species (Scheme 2). It was noted that the ^{1}H NMR and UV vis samples (stored in the dark) then remained unchanged over the period of several months, indicating that the resulting complex in the presence of a large excess of the ligated solvent, have excellent stability. Whilst this may be of synthetic importance, this ion selective reaction provides the possibility of reporting the presence of mercuric cations using SERS.

SERS studies of [Re(L2)(CO)$_3$Br] with metal salts

Given that [Re(L2)(CO)$_3$Br] can form highly ordered silver nanoparticle films, and has a very selective interaction with Hg^{2+} ions, this then is a suitable interaction to test whether this can be observed in the Raman response using of Ag@[Re(L2)(CO)$_3$Br]. A range metal perchlorate solutions (0.1 mL of a 1 mM acetonitrile) were introduced to freshly prepared AgNP@[Re(L2)(CO)$_3$Br] MeLLFs samples. In the majority of cases, including the common cations Co^{2+}, Ni^{2+}, Cu^{2+}, Zn^{2+}, Cd^{2+}, and Pb^{2+}, the Raman response from the surface remained unchanged (Supp. Figure 18). With the addition of Hg^{2+}, Fe^{2+} and Ag^{+} there was however a decrease in the scattering intensity from the surface, although in the latter two cases, no change in the form of the spectra was observed. With Hg^{2+} a notable change in the observed Raman fingerprint is also observed, with the appearance of significant shoulders at 490 and 530 cm^{-1} to the Re–C vibration at 510 cm^{-1}, and a relative increase in intensity in comparison with the 1034 cm^{-1} bpy ring-ring stretching mode. This is consistent with the abstraction of the bromide group from the Re center. The presence of Hg^{2+} also results in the appearance of an unassigned new broad vibration at 330 cm^{-1} (Figure 7).

Investigation of the Ag@[Re(L2)(CO)$_3$Br] SENS surfaces with acetonitrile solutions of the metal perchlorate salts similarly shows the Hg^{2+} selectivity. With the exception of Hg^{2+}, all of the metal perchlorate salt solutions investigated showed no visible change in the appearance of the surface. Hg^{2+} however caused a dramatic reduction in the overall rhenium complex SERS intensity (Figure 7). Analysis of the spectrum shows that the vibrational modes belonging to the complex are still present, specifically the Re–C stretch at 510 cm^{-1} and the ring breathing mode at 997 cm^{-1}. But the spectrum also shows additional intense bands at 380 and 920 cm^{-1} attributed to the C–CN bending and C–C stretching of acetonitrile. It is unclear whether this is a result of the proposed Hg^{2+} facilitated bromide removal and subsequent detachment of the complex or a result of solvent coordination into the vacant space, or the stripping, reduction and amalgamation of mercury with the surface, consistent with the observed aggregation in previous reports.[33]

An assessment was also made on the concentration limit of the system and the SENS film showed a response when exposed to 100 µl of a 0.01 mM Hg^{2+} solution, a ten fold increase in sensitivity compared to the AgNP@[Re(L2)(CO)$_3$Br] MeLLF. In a similar experiment, AgNP@[Re(L2)(CO)$_3$Br] SENS were screened with aqueous solutions of the metal perchlorate salts demonstrated that Hg^{2+} detection was also possible in water. The implications are that such platforms have potential for real-world

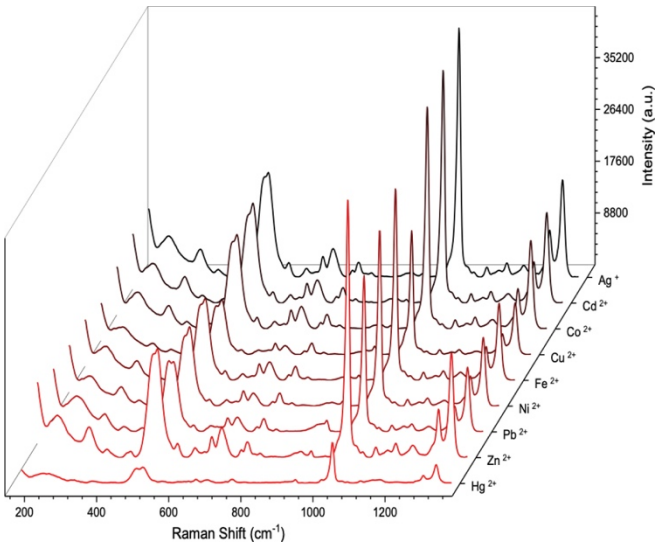

Figure 6 The SERS response of the Ag@[Re(L2)(CO)$_3$Br] SENS to metal perchlorate salts in acetonitrile.

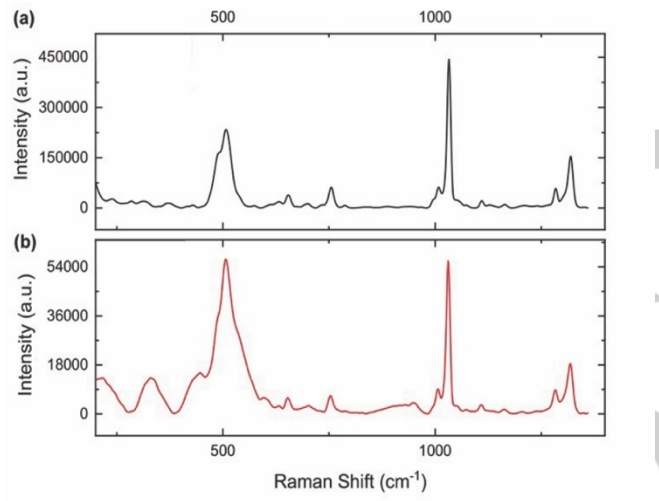

Figure 7. The SERS spectrum of a MeLLF formed using a 1 mM solution of (a) [Re(L2)(CO)$_3$Br]) and (b) the resulting spectrum after addition of a 1 mM solution of Hg(ClO$_4$)$_2$ excited at 785 nm.

testing as sensing is not hindered by solvent, unlike the luminescence response.

Conclusion

In summary, this paper reports a new approach for the fabrication of labelled interfacial silver nanoparticle films that can be employed for targeted SERS-based detection. Preliminary attempts using Ag@L2 MeLLFs show discriminate sensing of aqueous metal cations as shown by changes to the SERS response. Incorporating a rhenium carbonyl function introduces SERS active bands outside of biological spectral window, and abstraction of a coordinated bromide demonstrates a remarkable selectivity for Hg^{2+} with complexes of the form [Re(L)(CO)$_3$Br]. This is highlighted by the significant changes in the UV-vis, emission, and NMR spectra. [Re(L2)(CO)$_3$Br] binds to the AgNPs and successfully encourages the formation of both MeLLF and SENS that display a characteristic Raman fingerprint. The Hg^{2+} selectivity is translated to these Ag@[Re(L2)(CO)$_3$Br] interfacial films with both MeLLF and SENS analogues showing a SERS response to the presence of Hg^{2+} which is not seen with other metal cations. Furthermore, the SENS displays greater levels of sensitivity and sensing abilities in aqueous media. To the best of our knowledge, this is the first example where tethered Re(I) complexes have been used as both nanoparticle modifiers, causing interfacial positioning of the Ag nanoparticles to form films, as well as providing a label for SERS detection of mercuric salts. This provides proof of concept, and we are currently exploring whether there is wider application through appropriate ligand design to explore sensing of anionic and biologically relevant molecules.

Experimental Section

Instrumentation: ^{1}H and ^{13}C NMR spectra were recorded on a Bruker Avance III 400 using the solvent as an internal reference, electronic absorption spectra were recorded on an Agilent Carey 60 UV vis spectrometer, fluorescence experiments were recorded in aerobic conditions on an Agilent Carey Eclipse spectrophotometer. Electrospray mass spectra of dissolved samples, diluted in CH_3CN were recorded on a Shimadzu LCMS IT ToF instrument. Microanalyses were performed on a Vario MICRO Cube**.** Raman measurements were acquired using a an InVia System (Renishaw plc, Wooton-Under edge U.K.) using a 785 nm wavelength laser operating at 100% and 20 mW. Spectra of the interfacial films were taken using a 20x optic, taking 10 accumulations of 1 second exposures. Continuous scanning experiments were also conducted using a 20x optic, scanning from 200 to 3200 cm^{-1} using a 10 second exposure. Baseline correction was using an adaptive curve method and smoothing was done using triangular moving average.

Starting materials: All were used as received from the supplier. Laboratory grade solvents were used unless otherwise specified. DCM was dried by stirring overnight with anhydrous $MgSO_4$. 4-Hydroxymethyl-2,2'-bipyridine, 5-hydroxymethyl-2,2'-bipyridine,[42] 2,2'-bipyridin-5-ylmethyl)-4-(1,2-dithiolan-3-yl)pentanoate (L1), *fac*-Re(bipy)(CO)$_3$Br[43] and *fac*-Re(L1)(CO)$_3$Br[11] were prepared according to literature procedures.

Synthesis of L2: 2,2'-Bipyridin-4-ylmethyl)-4-(1,2-dithiolan-3-yl)pentanoate was prepared using an adapted procedure for the synthesis of L1.[11] 4-Hydroxymethyl-2,2'-bipyridine (0.100 g 0.537 mmol) and thioctic acid (0.1109 g, 0.537 mmol) were dissolved in dry DCM (45 ml) and stirred for 45 min at 0°C. DCC (0.1663 g, 0.806 mmol) and DMAP (0.198 g, 1.621 mmol) dissolved in dry DCM was then added and stirred for another hour at 0°C and then stirred for 24 h at room temperature. The resulting solution was washed with water and the organic residues were dried with $MgSO_4$. The solvent was then removed and then the product was purified with silica column chromatography, collecting the 1st major fraction (eluent 59:39:2 hexane: ethyl acetate: triethylamine) as a pale yellow oil. Yield 0.1344 g, 67%. ^{1}H NMR 300 MHz, $CDCl_3$ δ 1.43-1.54 (2H, m, CH_2), 1.64-1.73 (4H, m, 2CH_2), 1.81-1.93 (1H, m, CH_2), 2.36-2.46 (1H, m, CH_2), 2.44 (2H, t, J = 7.5 Hz, CH_2), 3.03-3.19 (2H, m, CH_2), 3.49-3.59 (1H, m, CH_2), 5.20(1H, s), 7.27 (1H, dd, J = 5.0, 1.8 Hz, CH_2, CH^5), 7.31 (1H, ddd, J = 7.6, 4.8, 1.2 Hz, $CH^{5'}$), 7.71 (1H, ddd, J = 7.6, 8.0, 1.8 Hz, $CH^{4'}$), 8.37 (1H, bs, CH^3), 8.40 (1H, ddd, J = 8.0, 1.8, 1.2 Hz, $CH^{3'}$), 8.66 (1H, dd, J = 5.0, 0.9 Hz, CH^6), 8.68 (1H, ddd, J = 4.8, 1.8, 0.9 Hz, $CH^{6'}$); ^{13}C NMR 100 MHz, $CDCl_3$ δ 24.6 (CH_2) 28.7 (CH_2), 33.9 (CH_2), 34.6 (CH_2),38.5 (CH_2), 40.2 (CH_2), 56.3 (CH), 64.4 (CH_2), 119.3 (CH), 121.2 (CH),122.0 (CH), 123.9 (CH),137.0 (CH), 146.0 (Q), 149.2 (CH), 149.5 (CH), 155.8 (Q), 156.5 (Q),

173.0 (Q); ES-MS: 375.2 $[M]^+$ Elemental analysis found (calculated): $C_{19}H_{22}O_2N_2S_2 \cdot 1$(acetone): C: 60.78 (61.08), H: 7.57 (6.45), N: 6.79 (7.39), S: 14.91 (14.82).

Synthesis of [Re(L2)(CO)$_3$Br]:[11] $[Re(CO)_5Br]$ (0.150 g, 0.370 mmol) refluxed in toluene 20 ml with L2 (0.160 g, 0.460 mmol) under a N_2 atmosphere for 18 h. The volume of solvent was reduced in volume (approx. 5 ml) causing the precipitation of the product, which was collected by filtration and washed 3 times with diethyl ether (3 x 10 ml) and allowed to dry. Yield 0.206 g, 72%. ^{1}H NMR 400 MHz, $CDCl_3$ δ 1.48-1.58 (2H, m, CH_2), 1.70-1.80 (4H, m, $2CH_2$), 1.88-1.98 (1H, m, CH_2), 2.45-2.52 (1H, m, CH_2), 2.52 (2H, t, *J* = 7.5 Hz, CH_2), 3.10-3.24 (2H, m, CH_2), 3.56-3.63 (1H,m, CH_2), 5.31(1H, s), 7.51 (1H, dd, *J* = 5.6, 1.6 Hz, CH_2, CH^5), 7.58 (1H, ddd, *J* = 7.6, 5.2, 1.2 Hz, $CH^{5'}$), 8.11 (1H, ddd, *J* = 7.6, 8.0, 1.6 Hz, $CH^{4'}$), 8.16 (1H, bs, CH^3), 8.25 (1H, d, *J* = 8.0 Hz, $CH^{3'}$), 9.07 (1H, d, *J* = 5.6 Hz, CH^6), 8.68 (1H, ddd, *J* = 4.8, 1.8, 0.9 Hz, $CH^{6'}$); ^{13}C NMR 100 MHz, $CDCl_3$ δ 24.6 (CH_2) 28.7 (CH_2), 33.8 (CH_2), 34.5 (CH_2),38.5 (CH_2),40.3 (CH_2), 56.3 (CH), 63.5 (CH_2), 121.5 (CH), 123.2 (CH),125.4 (CH), 127.3 (CH),138.9 (CH), 148.7 (Q), 153.4 (CH), 153.4 (CH), 155.4 (Q), 155.9 (Q), 172.7 (Q), 196.6 (Q); MS-ES: m/z 747 $[M+Na]^+$, 645 $[M-Br]^+$, 723 $[M-H]^-$. Elemental analysis found (calculated): $ReC_{22}H_{22}O_5N_2S_2Br$ $(NaBr)_{0.25}$: C: 35.16 (35.25), H: 2.74 (2.95), N: 3.94 (3.73), S: 8.73 (8.55). IR (KBr disk): 1739.3 (C=O), 1902.4, 2021.5 (3x ReC=O).

Metal Liquid-like films preparation:[44] Citrate-stabilized Ag nanoparticles[19] were prepared using $AgNO_3$ (45 mg) dissolved in Milli-Q H_2O (250 ml) and heated to reflux. A 1% aqueous sodium citrate solution (5 ml) was added over 30 s and the mixture left at reflux for 90 min before being cooled to room temperature. Vigorous stirring was used throughout. From this stock solution (4 ml) were mixed with the "modifying" species, a 0.1 mM acetone solution of either L2 or [Re(L2)(CO)$_3$Br], (100 µl) until a notable color change had occurred. A portion of dichloromethane (4 ml) was then added followed by vigorous shaking for 30 seconds or until a reflective emulsion was formed.

Surface-exposed nanosheets:[25] Citrate-stabilized Ag nanoparticles (4 ml) were mixed with the "modifying" species (100 µl) until a notable color change had occurred. A polystyrene/DCM solution (4 ml 0.06 g ml^{-1}) was added followed by vigorous shaking until a reflective emulsion was formed. The mixture was then transferred to a polypropylene petri dish and allowed to dry. The film was then cut away and transferred onto scotch tape.

Acknowledgements

This research has been supported by Lancaster University and Queen's University Belfast. The work has been completed the an EPSRC DTA PhD studentship for JNL, and a DELNI PhD studentship for HJM.

Keywords: SERS • Mercury • Sensors • Emission • Rhenium

Supporting Information:

The authors have cited an additional reference within the Supporting Information.[45]

[1] C. L. Haynes, A. D. McFarland, R. P. Van Duyne, *Anal. Chem.* **2005**, *77*.
[2] E. C. Le Ru, P. G. Etchegoin, *Principles of Surface-Enhanced Raman Spectroscopy: and related plasmonic effects*, Elsevier Science, **2008**.
[3] (a) S. L. Kleinman, R. R. Frontiera, A.-I. Henry, J. A. Dieringer, R. P. Van Duyne, *Phys. Chem. Chem. Phys.* **2018**, *15*, 21-36; (b) K. Kneipp, Y. Wang, H. Kneipp, L. T. Perelman, I. Itzkan, R. R. Dasari, M. S. Feld, *Phys. Rev. Lett.* **1997**, *78*, 1667-1670.
[4] H. Sohrabi, A. Hemmati, M. R. Majidi, S. Eyvazi, A. Jahanban-Esfahlan, B. Baradaran, R. Adlpour-Azar, A. Mokhtarzadeh, M. de la Guardia, *Trends Anal. Chem.* **2021**, *143*, 116344.
[5] (a) M. Arabi, A. Ostovan, Z. Zhang, Y. Wang, R. Mei, L. Fu, X. Wang, J. Ma, L. Chen, *Biosens. Bioelectron.* **2021**, *174*, 112825; (b) W. W. Y. Lee, V. A. D. Silverson, L. E. Jones, Y. C. Ho, N. C. Fletcher, M. McNaul, K. L. Peters, S. J. Speers, S. E. J. Bell, *Chem. Commun.* **2016**, *52*, 493-496; (c) D. Song, R. Yang, F. Long, A. Zhu, *J. Env. Sci.* **2019**, *80*, 14-34.
[6] J. L. Li, L. X. Chen, T. T. Lou, Y. Q. Wang, *ACS Appl. Mater. Interfaces* **2011**, *3*, 3936-3941.
[7] Z. Guo, A. O. Barimah, C. Guo, A. A. Agyekum, V. Annavaram, H. R. El-Seedi, X. Zou, Q. Chen, *Spectroc. Acta Pt. A-Molec. Biomolec. Spectr.* **2020**, *242*, 118747.
[8] (a) N. C. Fletcher, M. C. Lagunas, *Topics Organomet. Chem.* **2009**, *28*, 143-170; (b) H. Saeed, S. Sreedharan, J. Thomas, *Chem. Commun.* **2020**, *56*, 1464-1480; (c) C. Caporale, M. Massi, *Coord. Chem. Rev.* **2018**, *363*, 71-91; (d) Y. Yang, G. Liao, C. Fu, *Polymers* **2018**, *10*, 650.
[9] (a) A. N. Dosumu, S. Claire, L. S. Watson, P. M. Girio, S. A. M. Osborne, Z. Pikramenou, N. J. Hodges, *JACS Au* **2021**, *1*, 174-186; (b) A. J. Hallett, P. Christian, J. E. Jones, S. J. A. Pope, *Chem. Commun.* **2009**, 4278-4280.
[10] (a) F. C. M. Leung, A. Y. Y. Tam, V. K. M. Au, M. J. Li, V. W. W. Yam, *ACS Appl. Mater. Interfaces* **2014**, *6*, 6644-6653; (b) M.-J. Li, X. W. Liu, M.-J. Nie, Z.-Z. Wu, C.-Q. Yi, G.-N. Chen, V. W. W. Yam, *Organomet.* **2012**, *31*, 4459-4466.
[11] H. J. Montgomery, D. Pelleteret, S. E. J. Bell, N. C. Fletcher, *Inorg. Chem.* **2011**, *50*, 2738-2747.
[12] L. Pérez-Mirabet, S. Surinyach, J. Ros, J. Suades, R. Yáñez, *Mater. Chem. Phys.* **2012**, *137*, 439-447.
[13] K. V. Kong, Z. Lam, W. K. O. Lau, W. K. Leong, M. Olivo, *J. Am. Chem. Soc.* **2013**, *135*, 18028-18031.
[14] D. Lin, T. Gong, Z.-Y. Hong, S. Qiu, J. Pan, C.-Y. Tseng, S. Feng, R. Chen, K. V. Kong, *Anal. Chem.* **2018**, *90*, 7139-7147.
[15] P. G. Etchegoin, E. Le Ru, *Phys. Chem. Chem. Phys.* **2008**, *10*, 6079-6089.
[16] B. Vlčková, S. M. Barnett, T. Kanigan, I. S. Butler, *Langmuir* **2018**, *9*, 3234-3238.
[17] L. Faucher, E. F. Borra, A. M. Ritcey, *J. Nanosci. Nanotechnol.* **2008**, *8*, 3900-3908.
[18] Y. K. Xu, M. P. Konrad, W. W. Y. Lee, Z. Ye, S. E. J. Bell, *Nano Lett.* **2016**, *16*, 5255-5260.
[19] P. C. Lee, D. Meisel, *J. Phys. Chem.* **1982**, *86*, 3391-3395.
[20] (a) Y. Ma, D. Sikdar, Q. He, D. Kho, A. R. Kucernak, A. A. Kornyshev, J. B. Edel, *Chem. Sci.* **2020**, *11*, 9563-9570; (b) M. P. Cecchini, V. A. Turek, A. Demetriadou, G. Britovsek, T. Welton, A. A. Kornyshev, J. D. Wilton‐Ely, J. B. Edel, *Adv. Opt. Mater.* **2014**, *2*, 966-977; (c) M. Wang, Z. L. Zhang, J. Y. He, *Langmuir* **2015**, *31*, 12911-12919; (d) P. Wen, F. Yang, C. Ge, S. Li, Y. Xu, L.-A. Chen, *Nanotechnol.* **2021**, *32*, 395502.
[21] A. Stewart, S. Zheng, M. R. McCourt, S. E. J. Bell, *ACS nano* **2012**, *6*, 3718-3726.
[22] G. Socrates, *Infrared and Raman characteristic group frequencies: tables and charts*, John Wiley & Sons, **2004**.
[23] M. Muniz‐Miranda, *J. Raman Spec.* **2000**, *31*, 637-639.
[24] H. C. Garcia, R. Diniz, M. I. Yoshida, L. F. C. de Oliveira, *Crystengcomm* **2009**, *11*, 881-888.
[25] Y. Xu, M. P. Konrad, J. L. Trotter, C. P. McCoy, S. E. J. Bell, *Small* **2017**, *13*, 1602163.
[26] P. Wu, L.-B. Zhong, Q. Liu, X. Zhou, Y.-M. Zheng, *Nanoscale* **2019**, *11*, 12829-12836.
[27] B. Gworek, W. Dmuchowski, B. D. A.H., *Environ. Sci. Eur.* **2020**, *32*, 128.
[28] (a) Y. J. Ding, S. S. Wang, J. H. Li, L. X. Chen, *Trac-Trends Anal. Chem.* **2016**, *82*, 175-190; (b) J. Huber, K. Leopold, *Trac-Trends Anal. Chem.* **2016**, *80*, 280-292.
[29] A. A. Furletov, V. V. Apyari, A. V. Garshev, S. G. Dmitrienko, Y. A. Zolotov, *J. Anal. Chem.* **2017**, *72*, 1203-1207.
[30] S. Bothra, J. N. Solanki, S. K. Sahoo, *Sens. Actuators B-Chem.* **2013**, *188*, 937-943.
[31] A. Y. Olenin, A. S. Korotkov, *J. Anal. Chem.* **2021**, *76*, 721-727.

[32] G. V. Ramesh, T. P. Radhakrishnan, *ACS Appl. Mater. Interfaces* **2011**, *3*, 988-994.
[33] (a) M. K. Choudhary, S. Garg, A. Kaur, J. Kataria, S. Sharma, *Mater. Chem. Phys.* **2020**, *240*; (b) K. Farhadi, M. Forough, R. Molaei, S. Hajizadeh, A. Rafipour, *Sens. Actuators B-Chem.* **2012**, *161*, 880-885; (c) F. L. Mi, S. J. Wu, W. Q. Zhong, C. Y. Huang, *Chem. Phys. Phys. Chem.* **2015**, *17*, 21243-21253; (d) A. Nayal, A. Kumar, R. K. Chhatra, P. S. Pandey, *RSC Adv.* **2014**, *4*, 39866-39869; (e) M. Sengan, D. Veeramuthu, A. Veerappan, *Mater. Res. Bulletin* **2018**, *100*, 386-393; (f) P. Sharma, M. Mourya, D. Choudhary, M. Goswami, I. Kundu, M. P. Dobhal, C. S. P. Tripathi, D. Guin, *Sens. Actuators B-Chem.* **2018**, *268*, 310-318; (g) Z. G. Shen, Y. Q. Luo, Q. Wang, X. Y. Wang, R. C. Sun, *ACS Appl. Mater. Interfaces* **2014**, *6*, 16147-16155; (h) L. Zhan, T. Yang, S. J. Zhen, C. Z. Huang, *Microchim. Acta* **2017**, *184*, 3171-3178.
[34] S. Kraithong, J. Sirirak, K. Soisuwan, N. Wanichacheva, P. Swanglap, *Sens. Actuators B-Chem.* **2018**, *258*, 694-703.
[35] (a) L. Guerrini, R. A. Alvarez-Puebla, *ACS Omega* **2021**, *6*, 1054-1063; (b) W. Ji, L. F. Li, Y. Zhang, X. N. Wang, Y. Ozaki, *J. Raman Spec.* **2021**, *52*, 468-481.
[36] Y. Wu, T. T. Jiang, Z. Y. Wu, R. Q. Yu, *Biosens. Bioelectron.* **2018**, *99*, 646-652.
[37] X. F. Kong, C. H. Cheng, Q. F. Wang, M. W. Meng, C. S. Chen, X. J. Wang, S. Y. Huang, W. X. Gan, *Opt. Mater. Express* **2021**, *11*, 3015-3022.
[38] Y. B. Zhao, Y. Yamaguchi, Y. Ni, M. D. Li, X. M. Dou, *Spectrochim Acta Part A-Mol. Biomol. Spect.* **2020**, *233*.
[39] G. D. Xu, Q. J. Zhang, C. Gao, L. P. Ma, P. Song, L. X. Xia, *Microchem. J* **2021**, *168*.
[40] (a) K.-C. Chang, S.-S. Sun, M. O. Odago, A. J. Lees, *Coord. Chem. Rev.* **2015**, *284*, 111-123; (b) S. Hostachy, C. Policar, N. Delsuc, *Coord. Chem. Rev.* **2017**, *351*, 172-188.
[41] (a) L. Sacksteder, A. P. Zipp, E. A. Brown, J. Streich, J. N. Demas, B. A. Degraff, *Inorg. Chem.* **1990**, *29*, 4335-4340; (b) E. Wolcan, G. Torchia, J. Tocho, O. E. Piro, P. Juliarena, G. Ruiz, M. R. Féliz, *J. Chem. Soc. Dalton Trans.* **2002**, 2194-2202; (c) M. Wrighton, D. L. Morse, *J. Am. Chem. Soc.* **1974**, *98*, 998-1003.
[42] N. C. Fletcher, R. T. Brown, A. P. Doherty, *Inorg. Chem.* **2006**, *45*, 6132-6134.
[43] (a) E. Hevia, J. Perez, V. Riera, D. Miguel, S. Kassel, A. L. Rheingold, *Inorg. Chem.* **2002**, *41*, 4673-4679; (b) A. Klein, C. Vogler, W. Kaim, *Organometallics* **1996**, *15*, 236-244.
[44] J. A. Baldwin, B. Vlčková, M. P. Andrews, I. S. Butler, *Langmuir* **1997**, *13*, 3744-3751.
[45] E. Wolcan, G. Torchia, J. Tocho, O. E. Piro, P. Juliarena, G. Ruiz, M. R. Feliz, *J. Chem. Soc. Dalton Trans.* **2002**, 2194-2202.

Entry for the Table of Contents

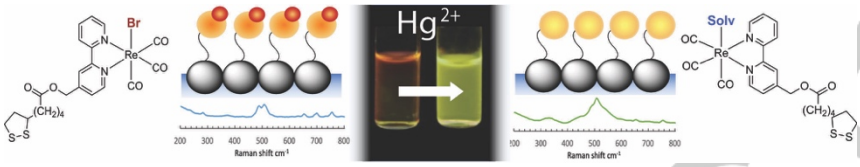

A rhenium carbonyl complex is shown to demonstrate the ability to form a stable silver nanoparticle lustrous film, whilst having a visible response to the presence of Hg^{2+} leading to new materials for “labelled” sensing using surface enhanced Raman spectroscopy.

Twitter: @LancUniChem